RSC Advances

ROYAL SOCIETY OF CHEMISTRY

www.rsc.org/advances

Kinetics and influence mechanism of mercury ion on papain catalytic activity

Xue-Ying Liu[a, b,]*, Hong-Yan Zeng[a,]*, Meng-Chen Liao[a], Bi Foua Claude Alain Gohi[a], Bo Feng[a]

[a] Biotechnology Institute, College of Chemical Engineering, Xiangtan University, Xiangtan 411105, Hunan, China

[b] Economical Forest Cultivation and Utilization of 2011 Collaborative Innovation Center in Hunan Province, Hunan Key Laboratory of Green Packaging and Application of Biological Nanotechnology, Hunan University of Technology, Zhuzhou 412007, China

*Corresponding Author

Hong-Yan Zeng

E-mail address: hongyanzeng99@hotmail.com; hyzeng@xtu.edu.cn

Address: School of Chemical Engineering, University of Xiangtan, Xiangtan 411105, Hunan, China

Tel.: 86-731-58298175

Fax: 86-731-58298167

Abstract

The effect of mercury ion on papain activity of the substrate casein was investigated. Mercury ion (Hg^{2+}) at low concentrations induced an increase of papain activity, but decreased it at high concentrations, confirming a typical hormesis phenomenon. Papain activity increased to a maximum of 111.03% at 10^{-6} mol/L Hg^{2+} concentration, but almost completely deactivated in above 10^{-4} mol/L Hg^{2+} concentration. The conformational changes in papain structure due to the interaction of Hg^{2+} and papain were studied by SRCD, ATR-FTIR and intrinsic fluorescence spectroscopies, and the enzyme catalytic behavior were studied by kinetic analysis. At up to 10^{-4} mol/L concentrations, Hg^{2+} significantly decreased the α-helix content of papain and increased random coil content so that the papain with lower affinity to substrate was nearly completely inactivated. On the contrary, papain activity increased with increase of the α-helix content and decrease of random coil when the Hg^{2+} concentration at 10^{-6} mol/L. There were different modification mechanisms of Hg^{2+} at different concentrations on papain activity. At 10^{-6} mol/L Hg^{2+} concentration, Hg^{2+} was exhibited as an efficacious activator, and the impact could classify into noncompetitive type. At 10^{-4} mol/L Hg^{2+} concentration, the inhibition of Hg^{2+} on papain was found to be a competitive and uncompetitive mixed type, and Hg^{2+} at the concentration bound to the enzyme molecule led the losing of enzyme activity. As a result, papain was of a detection limit of 10^{-4} mol/L and has a potential application for low doses of Hg^{2+} determination.

Keywords: Protease; Mercury ion; Enzyme activity; Biocatalysis; Irreversible modification; Kinetic parameters

1. Introduction

Due to rapid and incessant industrial development of china, heavy metal contaminants have been introduced into natural waters, soil and air. These metal contaminants, unlike organic pollutants, cannot be detoxified via degradation and thus persist in the ecosystem. They get into the human food chain from the environment causing hazardous effects on human, animal and plant organisms.[1-3] Certain metal ions are highly toxic, and the determination of traces of toxic heavy metals in these environmental pollutants has become very important. Among them, Hg^{2+} has attracted the most attention due to its strong toxicity and increasing level of its extended use in industrial processes.[4-6]

Mercury can be determined by atomic absorption spectrometry, X-ray fluorescence spectroscopy, high performance liquid chromatography and electrochemical methods. The disadvantages of the above methods are the complicated operation process and expensive equipments and skilled operation workers.[7] Heavy metals are well known as inhibitors on enzyme activity and the application of this phenomenon to the determination of these hazardous toxic elements by enzymes has received considerable attention and offers several advantages, such as relatively short response time, high sensitivity, selectivity and specificity. Most of these enzymes are cheap and does not require costly instruments and stringent requirements as these toxic substances bioassays. Thus, a lot of enzymes have been used for the inhibitive determination of traces heavy metal ions in environmental samples. Some enzymes such as papain, urease, glucose oxidase, xanthine oxidase have been used for the determination of Hg^{2+}.[1, 3, 4, 7-10] Since mercury is a soft acid and the residues containing thiol group are soft bases, Mercury targets the thiol-containing enzymes, irreversibly binding their

critical thiol groups, consequently leading to an inactivation of the enzyme.[11-13] So the inhibition of enzymatic activity by mercury may offer a good choice as a simple, rapid and sensitive screen test.

Papain (EC 3.4.22.2) is a highly stable enzyme, one of the proteolytic enzymes from papaya latex.[14] Papain is a cysteine protease consisted of 212 amino acid residues including 7 Cys residues and is stabilized by three disulfide bridges.[15, 16] Hg^{2+} (soft acid) had a strong bond with the cysteine residues in papain (soft base) resulting in irreversible inhibition of papain.[11, 17, 18] The papain assay has a wide pH for optimum activity, temperature stability and sensitiveness to heavy metals so that the papain assay was used to monitor heavy metals including Hg^{2+} in water environments [3, 13]. When enzymes are exposed for minutes to Hg^{2+}, there is an influence on the activity of enzyme such as tyrosine kinase, phospholipase C and Ca^{2+}-ATPase.[19, 20]

Hormesis is a rule rather than an exception, which represents an evolutionary-based adaptive response to environmentally induced disruption in homeostasis. Though the biphasic dose-response is a common result of experiments, the low dose data have been largely ignored. The hormesis phenomenon, low-dose stimulation followed by high-dose inhibition, is relatively commonly observed among classes of organisms including enzyme activity in response to various heavy metals.[21, 22] Hg^{2+} is one of the most hazardous heavy metals in the environment. Most of the studies are more concerned about the toxic effects of Hg^{2+} at high concentrations, and much less information is available about the effect of Hg^{2+} at low concentrations. For determining trace of mercury in waters, it is essential to investigate enzyme activity in response to different Hg^{2+} concentrations.

The principal aim of the present work was to evaluate the influence of Hg^{2+} on papain activity. The combination of SRCD, ATR-FTIR and intrinsic fluorescence spectroscopies as well as kinetics analysis was used to understand the structure-function relationship in the presence of Hg^{2+}. The present work would be useful to understand the interaction mechanism takes place between mercury and papain and it will be of potential applications as a bioindicator for heavy metals.

2. Materials and methods

2.1. Enzyme and reagents

Papain (EC3.4.22.2, ≥ 99%), bovine serum albumin (BSA), tyrosine and casein were purchased from Sigma Aldrich (Shanghai, China). All other reagents used were of analytical grade and without further purification. All solutions were made with redistilled and ion-free water.

2.2. Effect of Hg^{2+} on papain activity

Papain activity was measured as described in Guo et al..[23] Papain solution (1.0 mg/mL) was obtained by dissolving the enzyme in PBS buffer (0.1 mol/L, pH 7.0). Stock solution of $HgCl_2$ (0.1 mol/L) was prepared in the PBS buffer and it was diluted into the concentration varied from 10^{-9} to 10^{-2} mol/L for the assays of papain activity in the presence of Hg^{2+}. In the preliminary experiment, it was found that the reaction attained the equilibrium after 30 min (Fig. S1) that was the same as the equilibrium time described in Guo et al. literature.[23] So, the reaction time for the hydrolysis was set to 30 min. The papain solutions were initially added in the buffers at different Hg^{2+} concentrations, respectively. After 10 min at 40 ℃, 3.0 mL casein solution (2.0 mg/mL) was added into the mixture at 40 ℃ for 30 min before addition of

2.0 mL trichloroacetic acid (TCA) of 20% (by mass) to stop the reaction. The activity of papain was determined by a U-9100 spectrophotometer (Hitachi, Tokyo, Japan) at 275 nm. One unit of enzyme activity (U) was defined as 1μg tyrosine formed per minute at 40°C and pH 7.0. The relative activity (%) was the ratio of the enzyme activity in the PBS buffer at different Hg^{2+} concentrations and in the PBS buffer without Hg^{2+}.

2.3. ATR-FTIR and intrinsic fluorescence spectroscopies

ATR-FTIR spectra of the samples in the ATR cells were recorded on PE Spectrum One B instrument (Perkin-Elmer, Waltham, USA). Background was subtracted using the Opus software. Curve fitting was performed using Origin 9.0 and PeakFit v4.12 software. The tryptophan (Trp) fluorescence spectra were recorded using a LS55 spectrofluorimeter (Perkin-Elmer, Waltham, USA) at 25 ℃. The emission spectra were recorded in the range of 300~410 nm at 500 nm/min, 10 s after excitation, keeping the excitation constant at 288 nm, with slit widths of 5 nm for excitation and emission. Tryptophan ethyl ester was used as internal standard to correct the inner filter effect. The blank spectra without enzyme was subtracted from the sample spectra.

Papain (0.5 mg/mL) was equilibrated in the solutions with 0 (control), 10^{-6}, 10^{-5} and 10^{-4} mol/L concentrations of Hg^{2+} at 40 ℃ for 10 min, respectively, and then centrifuged at 3000 rpm (equal to g value 800) for 4 min. The supernatant was used for ATR-FTIR and fluorescence spectral measurements. Triplicate samples were analyzed and spectra for the triplicate runs were averaged and used as the final spectra data.

2.4. Synchrotron radiation circular dichroism (SRCD) spectroscopy

Samples were examined in circular demountable 0.0015 cm pathlength suprasil cells

(Hellma, Cumberland House, UK), which had been previously calibrated using interferometry methods.[24] At the 4B8 beamline of the Beijing Synchrotron Radiation Facility (BSRF, Beijing, China), 3 repeats of each of the protein samples were measured over the wavelength range from 280 to 165 nm at 5 ℃, using a 1 nm interval and a time constant of 5 s. At CD1 spectra were measured using an interval of 1 nm and dwell time of 2.1 s. Five repeats of each protein spectrum were measured from 260 to 172 nm at 25 ℃. Spectral data from both beamlines were processed using identical procedures with CDtool software, and secondary structure analyses were performed with CDPro software package (at http://lamar.colostate.edu/~sreeram/CDPro/main.html), which was consisted of three of the popular programs (SELCON3, CDSSTR and CONTINLL) for analyzing the protein CD spectra to determine the secondary structure fractions.[25, 26] The fitting was then performed using the three programs, and the best fitting procedure was based on root-mean-square deviation [RMSD(Exp-Calc)] and normalized root mean squared deviation [NRMSD(Exp-Cal)].

2.5. Kinetic measurements

Mercury effect was caused by tight binding of mercury to reactive –SH group in enzyme, and the effect was irreversible [11, 12, 17]. In order to investigate the irreversible modification by Hg^{2+} on papain activity, the kinetic model of substrate reaction during irreversible modification of enzyme activity described by Tsou was used to study the kinetics of papain by Hg^{2+}. And the model was not only suitable for inhibition kinetics, but also for activation kinetics.[27-29] For the kinetic method described by Tsou, it had been used in studies of inactivation of various enzymes by inhibitors.[30-32] However, most studies were focused on single inhibition [30-32] or single activation,[33-35] but little on both inactivation and activation of

an enzyme by a modificator. Here, the irreversible modification (inhibition/activation) of Hg^{2+} on papain activity was investigated. The reaction mechanism was considered in Scheme 1, where E, S, P and Y represent papain, substrate casein, product tyrosine and Hg^{2+}, respectively. EY, ES and EYS were the respective complexes.

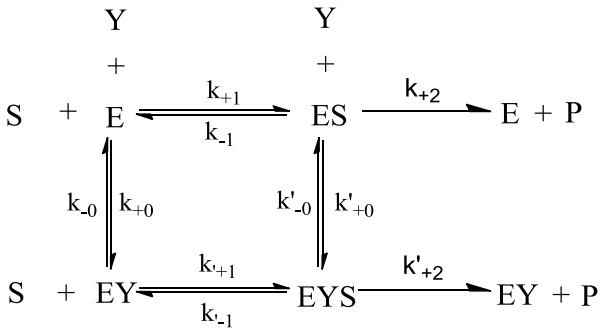

Scheme 1 Modification of papain by Hg^{2+} in the presence of substrate

As was usual the case $[S] \gg [E_0]$ and that the modification reactions were relatively slow compared with the setup of the steady-state of the enzymatic reaction. The concentration of the product formed can be written as [29],

$$[P]_t = v't + \frac{v - v'}{A}(1 - e^{-At}) \qquad (1)$$

$$A = \frac{k_0 K_m + k_0' [S]}{K_m + [S]} \qquad (2)$$

where $[P]_t$ was the concentration of the product formed at the reaction time t. A was the apparent rate constants. $[S]$ was the concentration of casein. v and v' were the reaction velocities of reaction in the absence and presence of Hg^{2+} at time t, respectively. K_m and K_m' were the Michaelis constants. k_0 and k_0' were the dissociation constants for the modifier with different forms of the enzyme, respectively. V_m and V_m' were maximum reaction velocities. When $v > v'$, the modifier Hg^{2+} was an inhibitor. When $v < v'$, the modifier Hg^{2+} was an activator. When the reaction time t was sufficiently long, the curves become straight lines and

the product concentration was written as [P_e]:

$$\frac{1}{[P_e]} = \frac{k_0 \cdot K_m}{V_{\mathrm{m}}} \cdot \frac{1}{[S]} + \frac{k_0'}{V_m} \qquad (3)$$

3. Results and discussion

3.1. Effect of Hg^{2+} on papain activity

The effect of Hg^{2+} concentration on papain activity was investigated and typical dose response phenomenon (hormesis) characterized by low-dose stimulation and high-dose inhibition was shown in Fig. 1. Hg^{2+} inhibited papain activity with a relative activity of 6.81% when Hg^{2+} concentration was $\geq 10^{-4}$ mol/L, but it was observed that stimulation of papain activity could occur at 10^{-6} mol/L of Hg^{2+} concentration and displayed the highest relative activity of 111.03%. There was no significant difference in papain activity, exposing to 10^{-10} ~10^{-7} and 10^{-5} mol/L of Hg^{2+} buffer. In order to see the effect of chloride ions, the effect of KCl on the enzyme activity was checked and there was no change in enzyme activity (data not shown). Thus the change in the activity observed was mainly due to the Hg^{2+} only. According to the results of the experiment, three different concentrations of Hg^{2+}, including 10^{-6}, 10^{-5} and 10^{-4} mol/L, were chosen to investigate the interactions between Hg^{2+} and papain activity.

3.2. Influence of Hg^{2+} on secondary structure of papain

It was possible that the change in enzyme activity observed in the buffer containing metal ion might be due to papain secondary structure changes. In the preliminary work, it was found that there was little difference between native papain and the papain samples exposed in 10^{-7} and 10^{-5} mol/L Hg^{2+} buffer from the spectra of ATR-FTIR and intrinsic fluorescence spectroscopy. So, the changes in the secondary structure of papain as a function of metal ion

concentration were determined by ATR-FTIR, intrinsic fluorescence and SRCD spectroscopies in the presence of the 10^{-6}, 10^{-5} and 10^{-4} mol/L Hg^{2+} concentrations.

3.3. ATR-FTIR

ATR-FTIR spectroscopy had been used extensively to study the changes in the secondary structure of protein. The amide I band between 1700~1600 cm^{-1} was the most useful for spectroscopic analysis of secondary structure of protein.[36] The original ATR-FTIR spectra of the individual papain sample in the 1800~900 cm^{-1} region were performed and the components peaks in the amide I region were determined by the curve fitting method and shown in Fig.2 and Table 1, which the individual component locations of papain secondary structure were assigned according to the methods by earlier studies.[36-38] Hg^{2+} had effect on the secondary structure of papain. Compared with the control, the papain exposed in 10^{-6} mol/L Hg^{2+} buffer exhibited an increase in α-helix and β-sheet and a decrease in β-turn and random coil. And the percentage of the aggregated structure in the papain was decreased from 8.40 to 5.33%. Again, there was no significant change in the structural features of the papain exposed in 10^{-5} mol/L Hg^{2+} buffer, implying that no major conformational changes occurred in the papain. However, in the presence of 10^{-4} mol/L Hg^{2+}, the α-helix content of the enzyme significantly decreased from 34.57 to 18.47%. The β-turn and random coil content rose from 19.19 to 22.38% and 23.47 to 31.69%, respectively. Especially, the papain dramatically decreased the contribution of the α-helix and increased the aggregated structure, but there was a very small decrease in β-sheet from 14.37 to 11.11 %. The results showed that the enzyme activity increased with the increase of α-helix content and decrease of intermolecular β-Sheet aggregate and random coil contents.

3.4. Intrinsic fluorescence spectroscopy

Intrinsic Fluorescence spectroscopy was used to investigate the perturbation of Trp residues in papain as a result of Hg^{2+} interaction with enzyme, and the fluorescence emission spectra of papain was shown in Fig. 3. Native papain in aqueous buffer showed a typical Trp peak with the maximum emission about 342 nm and the fluorescence was mainly due to the presence of five Trp residues in papain,[39] and the maximum emission of the control at 340.5 nm (Fig. 3a). Upon interaction of papain with Hg^{2+} of 10^{-6} mol/L concentration, the maximum fluorescence emission appeared a slightly blue shift (2 nm, Fig. 3c) with decrease in intensity compared with the control. This blue-shift could be attributed to the conformational changes in the vicinity of surface-exposed Trp residues, presumably because of internalization in a more hydrophobic environment. The papain exposed in 10^{-5} mol/L Hg^{2+} buffer did not alter the emission maximum with trifling decrease in intensity, implying that the papain basically maintained its native state in 10^{-5} mol/L Hg^{2+} concentration (Fig. 3b). In case of 10^{-4} mol/L Hg^{2+}, the markedly decrease in the emission intensity and a red shift of 7 nm in the emission maximum were found (Fig. 3d). It might be deduced that the internalized Trp residues in native state got partially exposed from a hydrophobic to a hydrophilic environment leading to partial unfolding of the molecule. In the last case, the Trp residues were buried inside a more polar protein surrounding, resulting in an inactive enzyme. All these data clearly suggested that the structural alteration of papain exposed in Hg^{2+} buffers induced the microenvironment change of the Trp residues.

3.5. SRCD spectroscopy

Far UV-CD spectra of papain in the presence of Hg^{2+} concentrations at 10^{-6}, 10^{-5} and

10^{-4} mol/L were showed in Fig.4. The spectrum of native papain (control) had a negative trough at 208 nm and a shoulder at 220 nm (Fig.4a). The effect of Hg^{2+} on papain was accompanied by only small change in the CD spectra of papain at low Hg^{2+} concentrations ($\leq$ 10^{-5} mol/L), whereas larger change in the conformation of papain molecule was observed at higher Hg^{2+} concentrations ($\geq 10^{-4}$ mol/L). All these signals were abolished following the papain exposed in 10^{-4} mol/L Hg^{2+} buffer, indicating the disruption of the native secondary structure and a loss of the rigid tertiary structure. The secondary structural features of the samples were summarized in Table 2. The change tend of each secondary structural content of papain using SRCD spectroscopy analyses matched with that by ATR-FTIR spectroscopy basically, indicating that the change tendency at different Hg^{2+} concentrations was defined and verified with each other. Deformation in papain secondary structure led to the change of the protein's native three-dimensional structure wherein the function of the protein could also be altered. Far UV-CD spectra revealed that papain-Hg^{2+} complex structure has certain deformation leading to the structural and functional change which might be considered as a significant factor in influencing its activity. The RMSD and NRMSD values fitted by IBasis6 in the SELCON3 program were smaller than 0.1, indicated the fitting method was well suitable to the secondary structure analyses of papain samples.[18, 40, 41] The α-helix content of native papain molecule was about 43.4% which was obtained through the CD spectrum data. Of the 2 domains in papain folding structure, the first domain of native papain had large α-helix content, while the secondary domain was mainly β-sheet and a lesser amount of α-helix.[42] Accompanied by slight enhancement of papain activity (Fig.1), the papain in the presence of 10^{-6} mol/L Hg^{2+} presented a modest increment for α-helix content, moreover,

slight decrease for the β-turn and random coil contents due to the binding of Hg^{2+}. The Hg^{2+} at 10^{-5} mol/L concentration had almost no effect on the secondary structural contents of papain. Nevertheless, exposing in 10^{-4} mol/L Hg^{2+}, the binding of Hg^{2+} to papain dramatically decreased the α-helix content and significant increased the β-sheet and random coil content leading to enzyme inactivation, while the β-turn changed very slightly compared with native papain. The binding of Hg^{2+} to papain was marked by significant changes in the shape and position of the far UV-CD spectra.

As suggested above, the results further confirmed that the enzyme activity increased with increase of α-helix content as well as decrease of random coil contents, and vice versa. It was important to note that papain activity could be influenced not just by active site geometry but also by domain packing property. In virtue of similar enzyme activity and secondary structure to native papain, the papain exposed in 10^{-5} mol/L Hg^{2+} buffer was eliminated for further kinetic experiments.

3.6. Kinetic constants

The kinetic parameters, K_m and V_{max}, of the papain were calculated from the Lineweaver-Burk and Michaelis-Menten models in presence of different Hg^{2+} (10^{-6} and 10^{-4} mol/L) and substrate casein (0.2, 0.4, 0.6, 0.8, 1.0, 1.6 and 2.0 mg/mL) concentrations. Lineweaver-Burk reciprocal plots of the samples were shown in Fig. S2. For the papain exposed in 10^{-6} mol/L Hg^{2+} buffer, the V_{max} value increased from 0.1281 mg/min for the control to 0.1400 mg/min, while K_m decreased from 2.3247 for the control to 0.9144 mg/mL. The decrease in K_m indicated that the papain exposed in the low-dose Hg^{2+} (10^{-6} mol/L) had an apparent higher affinity for its substrate than that of the control, and the V_{max} value was

therefore greater than that of the control. Table 1 and 2 showed that Hg^{2+} at 10^{-6} mol/L concentration increased the α-helix content of the papain, and it seemed to be related to the decrease of the random coil for remaining structures content. On the contrary, the V_{max} value of the papain exposed in 10^{-4} mol/L Hg^{2+} buffer reduced to 0.0864 mg/min, while K_m climbed to 2.4288 mg/mL. Hg^{2+} at 10^{-4} mol/L concentration was able to weaken the affinity for the substrate by decreasing α-helix content and enhancing random coil. These results suggested that the conformational change induced by Hg^{2+} led to a change in the affinity of the papain for the substrate.

3.7. Kinetics properties of papain in the presence of Hg^{2+}

The time course of hydrolysis of the substrate at 10^{-6} and 10^{-4} mol/L Hg^{2+} concentrations was shown in Fig. 5. For the substrate hydrolysis in the presence of Hg^{2+}, the rate increased with increasing substrate concentration, while the slope of the asymptote increased with increasing substrate concentration. The reaction progress curves of the control were linear over a lengthy period of time. The results analyzed by Tsou's method [29] suggested that Hg^{2+} at 10^{-6} mol/L concentration had a stimulating effect on enzyme activity, but Hg^{2+} at 10^{-4} mol/L concentration had an inhibitory effect. According to Eq. (1), the exponential linearized expressions had been achieved using least square fitting method by all data in Fig. 5. The kinetic parameters of the model were shown in Table 3. The results showed that the calculated the correlation coefficients R^2 were greater than 0.9891, indicating that the kinetic model could well describe the substrate hydrolysis during papain binding to Hg^{2+}. According to Eq. (3), the plot of 1/ [P_e] against 1/[S] gave a straight lines. The values of k_0 and k_0' were calculated, respectively, and listed in Table 3.

The *v* value of native papain was lesser than the *v'* value of papain exposed in 10^{-6} mol/L Hg^{2+} buffer, indicating that the Hg^{2+} could stimulate papain activity. Furthermore, The values of dissociation constant k_0 and k_0' could be obtained, and the value of k_0 (0.1509) was 10 times as much as that of k_0' (0.0150). It displayed that there was a binding of Hg^{2+} to both native enzyme (E) and enzyme-substrate complex (EY). The binding of Hg^{2+} to papain had two existing forms, EY and EYS, and EYS was more than EY. The apparent rate constant *A* was independent of [*S*] from data of Table 3, implying that Hg^{2+} at 10^{-6} mol/L concentration was noncompetitive activator for enzyme and activation had nothing to do with substrate concentration. The results strongly indicated that the amino-acid residues responsible for the binding interactions of Hg^{2+} to enzyme mainly located outside the active center of papain and induced the small conformation change of the residues leading increase of enzyme activity.

At 10^{-4} mol/L Hg^{2+} concentration, the *v* value was higher than the *v'* value, revealing Hg^{2+} was an inhibitor for papain. The values of k_0 (0.0634) and k_0' (0.0344) showed that Hg^{2+} binding papain had two existing forms, EY and EYS. A plot of 1/*A* versus [*S*] gave a nearly liner (R^2 0.9938), and *A* value increased with increasing substrate concentration [*S*], implying Hg^{2+} at 10^{-4} mol/L concentration was competitive inhibitor for papain. At the same time, it could be seen that Hg^{2+} at 10^{-4} mol/L concentration could combine with both native enzyme (E) and enzyme-substrate complex (ES) for forming EY and EYS, respectively, and it displayed a competitive and uncompetitive mixed type mechanism. From the $k_0 \approx 2k_0'$, it was found that the binding of Hg^{2+} to papain mainly occurred at the amino-acid residues from the active site of papain, and other outside the active site.

4. Conclusion

The study demonstrated that there were significant impacts of Hg^{2+} on papain, where the papain activity in the hydrolysis of casein was increased by Hg^{2+} at low concentrations but inhibited at high concentrations, which indicated the occurrence of a hormetic phenomenon. The strongest inhibition effect was observed when Hg^{2+} concentration was up to 10^{-4} mol/L, whereas mild activation was 10^{-6} mol/L. So, the lowest detection limit for papain was 10^{-4} mol/L Hg^{2+} concentration. The results showed that papain was suitable for the determination of Hg^{2+} in environmental analysis. The fundamental correlations between the structure of papain and its activity were clarified. The three-dimensional structure of the papain exposed in Hg^{2+} buffers was determined by ATR-FTIR, SRCD and intrinsic fluorescence spectroscopies. The papain exposed in 10^{-6} mol/L Hg^{2+} buffer had increase in α-helix and decrease in random coil, but the papain exposed in 10^{-4} mol/L Hg^{2+} buffer had increase in random coil but decrease in α-helix. The enzyme activity increased with the increase of α-helix content and decrease of random coil contents, and vice versa. At 10^{-6} mol/L Hg^{2+} concentration, the binding sites of the modifier with papain were basically situated at outside of active site of papain, where Hg^{2+} might induce change of enzyme conformation leading to increase in affinity for substrate and papain activity. At 10^{-4} mol/L Hg^{2+} concentration, the modifier bonded with the amino-acid residues within and outside active center of papain, and Hg^{2+} shifted the three-dimensional structure of papain conducing toward decrease in affinity for substrate and occurrence of strong inhibition on papain activity. It indicated that there was difference between the modification mechanisms of Hg^{2+} on papain activity at 10^{-4} mol/L and 10^{-6} mol/L concentrations.

Acknowledgments

This work is supported by National Natural Science Foundation of China (21105085, 31270988), Hunan Provincial Natural Science Foundation of China (No. 2015JJ2133), Scientific Research Fund of Hunan Provincial Education Department (13B120) and Economical Forest Cultivation and Utilization of 2011 Collaborative Innovation Center in Hunan Province [(2013) 448].

References

1. M. R. Guascito, C. Malitesta, E. Mazzotta and A. Turco, *Sensors and Actuators B: Chemical*, 2008, **131**, 394-402.
2. C. M. Jonsson, L. C. Paraiba and H. Aoyama, *Ecotoxicology*, 2009, **18**, 610-619.
3. Y. Shukor, N. A. Baharom, F. A. Rahman, M. P. Abdullah, N. A. Shamaan and M. A. Syed, *Analytica Chimica Acta*, 2006, **566**, 283-289.
4. F. Kuralay, H. Özyörük and A. Yıldız, *Enzyme and Microbial Technology*, 2007, **40**, 1156-1159.
5. P. Mahato, S. Saha, P. Das, H. Agarwalla and A. Das, *RSC Advances*, 2014, **4**, 36140-36174.
6. M. Govindhan, B.-R. Adhikari and A. Chen, *RSC Advances*, 2014, **4**, 63741-63760.
7. Y. Yang, Z. Wang, M. Yang, M. Guo, Z. Wu, G. Shen and R. Yu, *Sensors and Actuators B: Chemical*, 2006, **114**, 1-8.
8. T. Krawczyński vel Krawczyk, M. Moszczyńska and M. Trojanowicz, *Biosensors and Bioelectronics*, 2000, **15**, 681-691.
9. M. S. Mondal and S. Mitra, *Journal of Inorganic Biochemistry*, 1996, **62**, 271-279.
10. C. Chen, Q. Xie, D. Yang, H. Xiao, Y. Fu, Y. Tan and S. Yao, *RSC Advances*, 2013, **3**, 4473-4491.
11. M. J. Ram ŕez-Bajo, P. de Atauri, F. Ortega, H. V. Westerhoff, J. L. Gelp ŕ J. J. Centelles and M.

Cascante, *PloS one*, 2014, **9**, e80018.

12. R. Sharma, in *Enzyme Inhibition and Bioapplications*, ed. R. R. Sharma, InTech, Rijeka, 2012, DOI: doi: 10.5772/39273.

13. M. Shukor, N. Masdor, N. Baharom, J. Jamal, M. Abdullah, N. A. Shamaan and M. Syed, *Applied biochemistry and biotechnology*, 2008, **144**, 283-291.

14. H.-L. Nie, T.-X. Chen and L.-M. Zhu, *Separation and Purification Technology*, 2007, **57**, 121-125.

15. E. Amri and F. Mamboya, *American Journal of Biochemistry & Biotechnology*, 2012, **8**.

16. P. Kaul, H. Sathish and V. Prakash, *Food/Nahrung*, 2002, **46**, 2-6.

17. I. J. Kade, *Journal of biomedicine & biotechnology*, 2012, **2012**, 924549.

18. P. Pancoska and T. A. Keiderling, *Biochemistry*, 1991, **30**, 6885-6895.

19. B. Burlando, M. Bonomo, E. Fabbri, F. Dondero and A. Viarengo, *Cell Calcium*, 2003, **34**, 285-293.

20. B. Burlando, V. Magnelli, I. Panfoli, E. Berti and A. Viarengo, *Cellular Physiology and Biochemistry*, 2003, **13**, 147-154.

21. C. R. Wang, Y. Tian, X. R. Wang, H. X. Yu, X. W. Lu, C. Wang and H. Wang, *Chemosphere*, 2010, **80**, 965-971.

22. Y. Zhang, G. Shen, Y. Yu and H. Zhu, *Environmental pollution*, 2009, **157**, 3064-3068.

23. Y. Guo, Z. Wang, W. Qu, H. Shao and X. Jiang, *Biosensors & bioelectronics*, 2011, **26**, 4064-4069.

24. A. J. Miles, F. Wien, J. G. Lees and B. Wallace, *Spectroscopy: An International Journal*, 2005, **19**, 43-51.

25. N. Sreerama and R. W. Woody, *Methods in enzymology*, 2004, 318-350.

26. B. Wallace, J. Lees, A. Orry, A. Lobley and R. W. Janes, *Protein science*, 2003, **12**, 875-884.

27. P. B. Chock, C. Huang, C. Tsou and J. Wang, *Journal*, 1988.

28. A. G. McDonald and K. F. Tipton, *eLS*, 2012.

29. C. Tsou, *Advances in Enzymology and Related Areas of Molecular Biology, Volume 61*, 1988, 381-436.

30. Q.-X. Chen, Z. Zhang, X.-W. Zhou and Z.-L. Zhuang, *The international journal of biochemistry & cell biology*, 2000, **32**, 717-723.

31. J.-C. Lin, Q.-X. Chen, X.-L. Xie, Z.-L. Zhuang, Y. Shi and Q.-S. Huang, *Journal of Experimental Marine Biology and Ecology*, 2006, **339**, 30-36.

32. Z.-X. Wang, H.-B. Wu, X.-C. Wang, H. Zhou and C.-L. Tsou, *Biochem. J*, 1992, **281**, 285-290.

33. Y.-D. Park, Y. Yang, Q.-X. Chen, H.-N. Lin, Q. Liu and H.-M. Zhou, *Biochemistry and cell biology*, 2001, **79**, 765-772.

34. J. WU and Z. WANG, *Biochem. J*, 1998, **335**, 181-189.

35. J.-J. Xie, Q.-X. Chen, Q. Wang, K.-K. Song and L. Qiu, *Pesticide biochemistry and physiology*, 2007, **87**, 9-13.

36. J. Kong and S. Yu, *Acta Biochimica et Biophysica Sinica*, 2007, **39**, 549-559.

37. P. R. Palaniappan and V. Vijayasundaram, *Infrared Physics & Technology*, 2009, **52**, 32-36.

38. X. Zhao, F. Chen, W. Xue and L. Lee, *Food Hydrocolloids*, 2008, **22**, 568-575.

39. C. R. Llerena-Suster, C. José, S. E. Collins, L. E. Briand and S. R. Morcelle, *Process Biochemistry*, 2012, **47**, 47-56.

40. W. C. Johnson, *Proteins: Structure, Function, and Bioinformatics*, 1999, **35**, 307-312.

41. N. Sreerama, S. Y. Venyaminov and R. W. Woody, *Protein Science*, 1999, **8**, 370-380.

42. A. Szabó, M. Kotormán, I. Laczkó and L. M. Simon, *Process Biochemistry*, 2009, **44**, 199-204.

Figure legend

Fig.1 Effect of Hg^{2+} concentration on papain activity

Fig.2 Original FTIR spectra and individual Gaussian bands of papain in amide I region

------: Original FTIR spectra (upper); —: individual Gaussian bands (bottom)

(a): Control; (b): 10^{-4} mol/L Hg^{2+}; (c): 10^{-5} mol/L Hg^{2+}; (d): 10^{-6} mol/L Hg^{2+}.

Fig. 3 Fluorescence emission spectra of papain in different Hg^{2+} concentrations

(a): Control; (b): 10^{-5} mol/L Hg^{2+}; (c): 10^{-6} mol/L Hg^{2+}; (d): 10^{-4} mol/L Hg^{2+}.

Fig. 4 Far UV-CD spectra of papain exposed in different Hg^{2+} concentrations

(a): Control; (b): 10^{-5} mol/L Hg^{2+}; (c): 10^{-6} mol/L Hg^{2+}; (d): 10^{-4} mol/L Hg^{2+}.

Fig. 5 Time course of casein hydrolysis reaction by papain at different concentrations of Hg^{2+} and substrate

A: Control; B: 10^{-6} mol/L Hg^{2+}; C: 10^{-4} mol/L Hg^{2+}.

·····: Prediction; ■: Experiment.

1: 0.2 mg/mL casein; 2: 0.4 mg/mL casein; 3: 0.6 mg/mL casein; 4: 0.8 mg/mL casein; 5: 1.0 mg/mL casein.

1 Fig. 1.

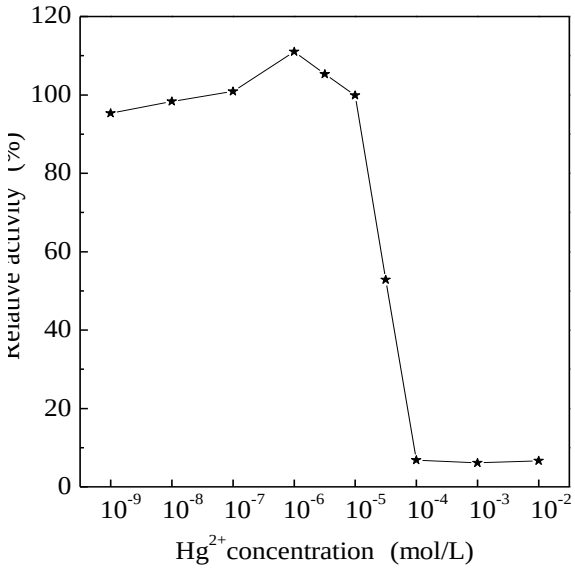

2

1 Fig.2.

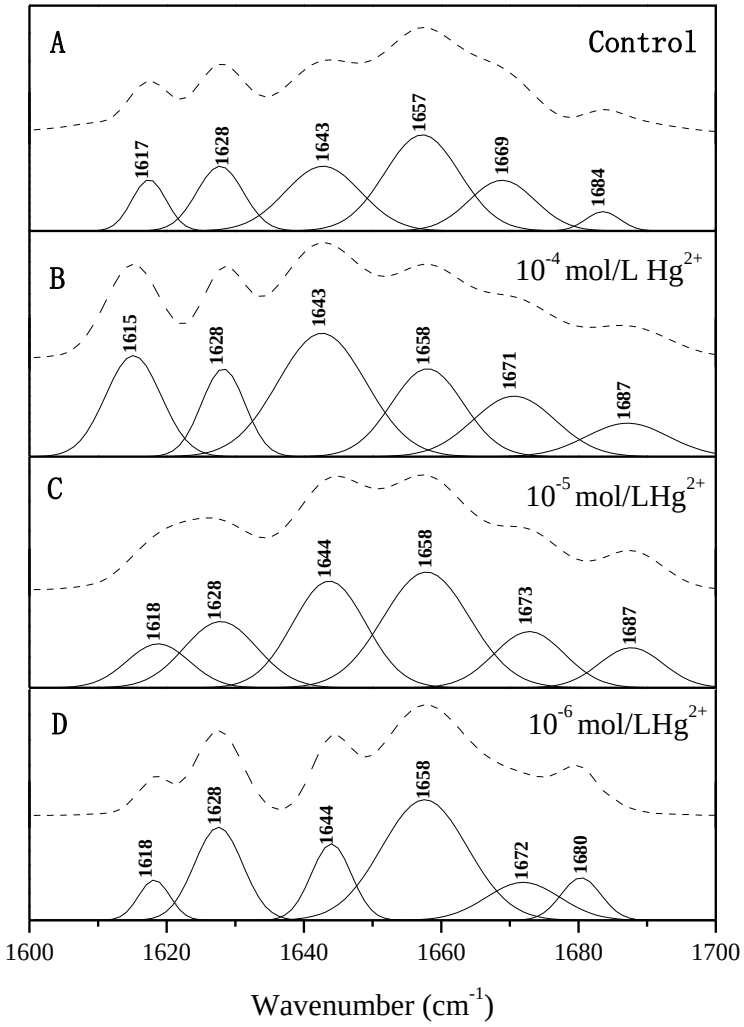

2

3

Fig. 3.

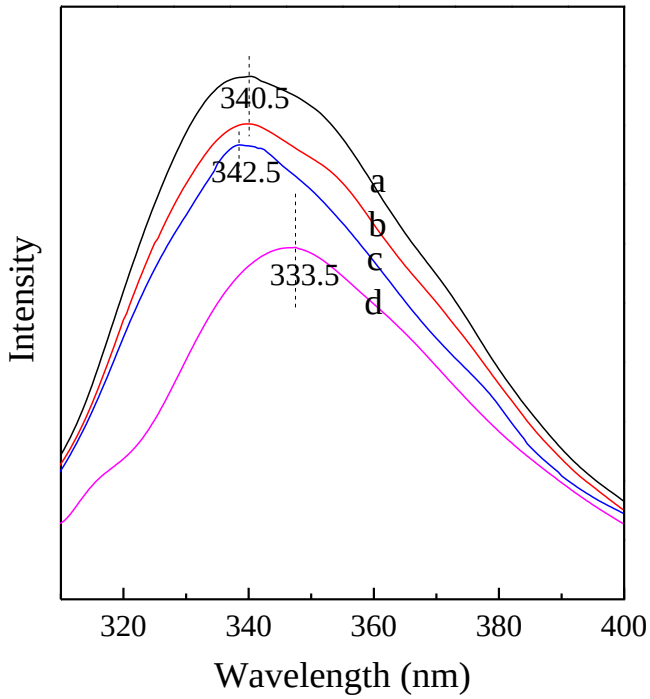

1 Fig. 4.

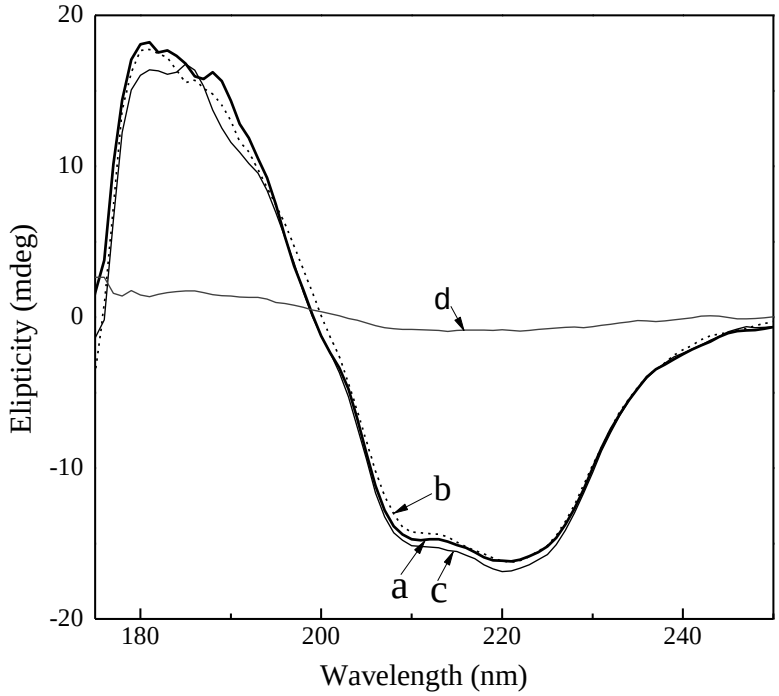

2

1 Fig. 5.

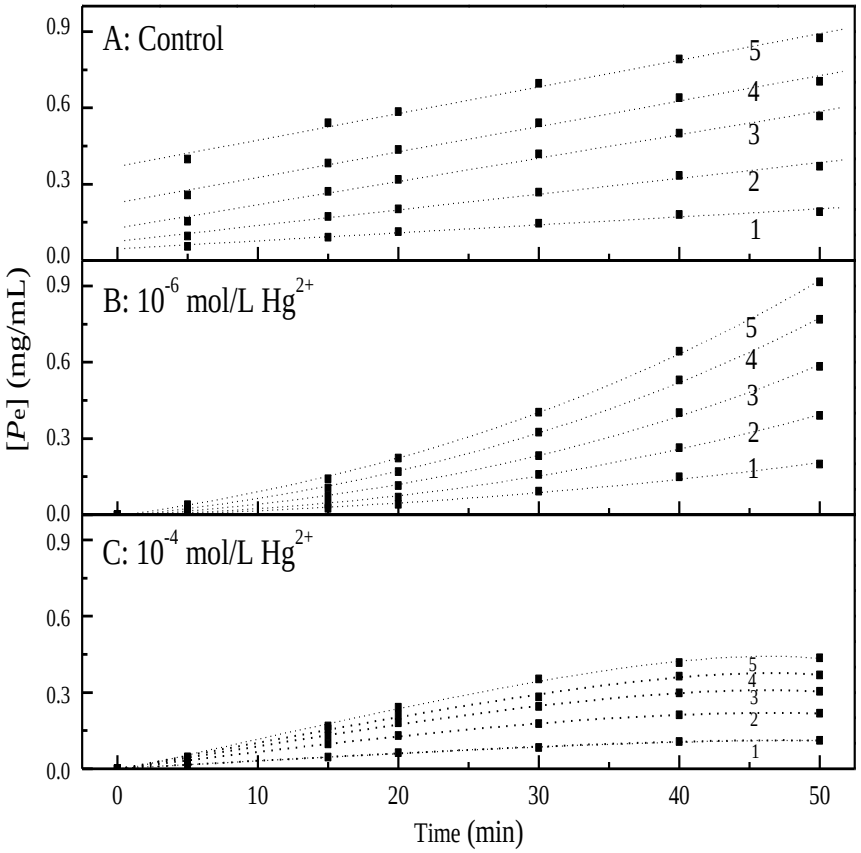

2

Table1 Secondary structure areas and assignments in amide I infrared bands of the papain in different Hg^{2+} concentrations

Second structure	Hg^{2+} concentration (mol/L)							
	Control		10^{-6}		10^{-5}		10^{-4}	
	Peak centers (cm^{-1})	Areas (%)	Peak centers (cm^{-1})	Areas (%)	Peak centers (cm^{-1})	Areas (%)	Peak centers (cm^{-1})	Areas (%)
Intermolecular β-sheet aggregates	1617	8.40	1618	5.33	1618	8.62	1615	16.35
β-Sheet	1628	14.37	1628	18.96	1628	15.15	1628	11.11
α-Helix	1657	34.57	1658	43.73	1658	31.46	1658	18.47
Random coil	1643	23.47	1644	12.95	1644	24.44	1643	31.69
β-Turn	1669 1684	19.19	1672 1680	19.03	1673 1687	20.33	1671 1687	22.38

* The reactions were performed at 40 ℃, pH 7.0 for 30 min, 0.5 mg/mL papain Tris-HCl solution was equilibrated in 0 (control), 10^{-6}, 10^{-5} and 10^{-4} mol/L concentrations of Hg^{2+} at 25 ℃ for 10 min, and then centrifuged at 3000 rpm (equal to g value 800) for 4 min.The supernatant was used to determine the structure changes of the treated papain. The papain without Hg^{2+} treated was used as the control. All the samples were determined three times and the data obtained from the triplicate runs were averaged and used as the final result. The contribution of the individual components of the secondary structure of papain in Hg^{2+}- PBS buffer was based on the reference [39].

Table2 Secondary structure contents of papain in different Hg^{2+}concentrations by CD spectroscopy

Hg^{2+} concentration (mol/L)	Second structure (%)*							
	H(r)	H(d)	α-helix	S(r)	S(d)	β-sheet	β-turn	Unrd
Control	28.2	15.2	43.4	5.3	7.4	12.7	16.0	27.2
10^{-6}	32.2	16.3	48.5	4.3	6.1	10.4	15.0	26.1
10^{-5}	27.4	14.5	41.9	5.4	7.4	12.8	17.1	28.2
10^{-4}	1.8	2.4	4.2	27.8	12.2	40.0	19.6	36.2

*The secondary structure fraction results of papain were obtained by the SELCON3 program using the IBasis6 in the wavelength range between 185-240 nm. The secondary structures are: H(r): regular α-helix; H(d): distorted α-helix; S(r): regular β-sheet; S(d): distorted β-sheet; Unrd: random coil.

Table 3 Kinetic parameters and dissociation constant of papain in casein hydrolysis

Hg^{2+} concentration (mol/L)	Casein concentration (mg/mL)	A (mg/mL)	v' (mg/min)	v (mg/min)	$[P_e]$ (mg/mL)	R^2	k_0	k_0'
Control	0.2	-	0.0031	0.0031	0.1967	0.9891	-	-
	0.4	-	0.0062	0.0062	0.3820	0.9951		
	0.6	-	0.0092	0.0092	0.5640	0.9953		
	0.8	-	0.0100	0.0100	0.7050	0.9952		
	1.0	-	0.0105	0.0105	0.8300	0.9959		
10^{-6}	0.2	0.0092	0.0124	0.0031	0.1984	0.9971	0.1509	0.0150
	0.4	0.0153	0.0182	0.0062	0.3878	0.9990		
	0.6	0.0143	0.0280	0.0092	0.5793	0.9994		
	0.8	0.0136	0.0235	0.0100	0.7604	0.9996		
	1.0	0.0081	0.0590	0.0105	0.8843	0.9999		
10^{-4}	0.2	0.0334	0.0030	0.0031	0.1069	0.9996	0.0634	0.0344
	0.4	0.0503	0.0059	0.0062	0.2123	0.9997		
	0.6	0.0643	0.0089	0.0092	0.2994	0.9994		
	0.8	0.0885	0.0099	0.0100	0.3645	0.9990		
	1.0	0.1004	0.0104	0.0105	0.4509	0.9989		

* The reactions were performed at 40 ℃, pH 7.0 for 30 min, 1.0 mg/mL papain Tris-HCl solution in different concentrations of Hg^{2+} ion. Every group test was run three times and the mean values were used as the final test results.